JOM, Vol. 76, No. 3, 2024
https://doi.org/10.1007/s11837-023-06361-w
© 2024 Crown

Effect of Annealing Temperature and Time on the Magnetic Properties and Magnetic Anisotropy of a Temper-Rolled, Semi-processed Non-oriented Electrical Steel

YOULIANG HE ,[1,3] RUBY ZHANG,[1] TIHE ZHOU,[2] HADEN LEE,[2] CHAD CATHCART,[2] and PETER BADGLEY[2]

1.—CanmetMATERIALS, Natural Resources Canada, Hamilton, Ontario L8P 0A5, Canada. 2.—Stelco Inc., Hamilton, Ontario L8L 8K5, Canada. 3.—e-mail: youliang.he@nrcan-rncan.gc.ca

The effect of final annealing temperature and time on the core loss, magnetic permeability, and magnetic anisotropy of a temper-rolled, semi-processed 0.5 wt.% Si non-oriented electrical steel was investigated. The magnetic properties of the steel sheets at 50–400 Hz and 0.5–1.50 T were measured by the Epstein frame method on strips cut along both the rolling (RD) and transverse directions (TD). Optimal magnetic properties were obtained when the annealing temperature was at 800–825°C, and the annealing time was 2–4 h. Relatively large magnetic anisotropy between the RD and TD was observed in samples after recrystallization ($\sim$ 10% in core loss and $\sim$ 70% in relative permeability), while deformed and non-recrystallized samples showed small anisotropy in magnetic properties. Regardless of the processing state of the steel, i.e., temper-rolled, recovered, or recrystallized, the core loss followed quadratic polynomial functions with respect to both the frequency and magnetic flux density, while the relative magnetic permeability followed cubic polynomial functions with respect to both the frequency and magnetic flux density. The microstructure and texture of selected samples were characterized by electron backscatter diffraction, which revealed the correlations between the magnetic properties of the steel and the microstructure and texture.

INTRODUCTION

Decarbonization through electrification has been recognized as an effective pathway to slow climate change and mitigate global warming caused by burning fossil fuels.[1] The generation of electricity from clean and renewable sources, e.g., wind, hydro, solar thermal power, tide, etc.,[2] and the use of electricity to drive electrical machines (e.g., electric vehicles, appliances, power tools, etc.), all rely on the use of non-oriented electrical steel (NOES) to fabricate lamination cores for the generators and electric motors. NOES is normally either fully processed which can be used directly without further processing, or semi-processed which requires final annealing by the user (usually after the steel sheets are cut into laminates).[3] Fully processed electrical steel must possess the required microstructure and texture to meet the specifications on magnetic properties, e.g., low core loss and high magnetic permeability, before it is delivered to the final user. Semi-processed NOES is usually subjected to a temper-rolling process (skin pass) before it is delivered to the user. Temper rolling increases the strip flatness, improves surface finish, accuracy, and mechanical properties for downstream processing, and eliminates defects such as edge wrinkles. After temper rolling, a final annealing step is always needed to achieve optimal magnetic properties in the lamination core. Proper operational conditions for the final annealing may be recommended by the steel manufacturer or determined by the final user. Although the thickness reduction rate of temper rolling is usually small (2–10%), the plastic deformation (normally with tension)[4] plays a crucial role in determining the microstructure, texture, and magnetic properties of the steel after final annealing.

(Received August 1, 2023; accepted December 20, 2023; published online January 12, 2024)

It is well known that all the thermomechanical processing steps employed to produce NOES sheets, from casting, hot rolling, and cold rolling to annealing, will influence the final microstructure, texture, and magnetic properties of the steel. Many papers can be found in the literature addressing the optimization of the final magnetic properties of NOES in all the thermomechanical processing steps.[5–12] However, even if the electrical steel sheets were produced to possess very good magnetic properties, the common lamination core manufacturing processes (e.g., stamping, interlocking, assembling, etc.) may deteriorate these properties, since they may induce stress, heat, and microstructure/texture changes in the material, thus affecting the magnetic properties of the lamination core.[13] As a result, the lamination core is preferably annealed after it is manufactured, which not only releases the stresses induced in the manufacturing processes but may also improve the final magnetic properties by optimizing the microstructure and texture through recrystallization.

Semi-processed NOES is an alternative electrical steel type which is normally more cost-effective to produce than fully processed NOES, since the final annealing process is not performed in the steel manufacturing stage. Semi-processed NOES is usually delivered to the final user after temper rolling, and always needs a final annealing treatment to release the stresses generated during temper rolling. Annealing after temper rolling may also result in significant changes in the microstructure and texture, since the plastic deformation during temper rolling induces stored energy in the microstructure, which provides the driving force for recovery and recrystallization.[14] The final annealing may lead to very different microstructures and textures (and thus magnetic properties) from the steel after temper rolling. While there is plenty of literature addressing the processing of fully processed NOES, the investigations of semi-processed NOES are much fewer.[15,16] Several papers have investigated the effect of the temper-rolling reduction rate,[16,17] tension,[18] and the final annealing conditions[19] on the magnetic properties of temper-rolled NOES. Nevertheless, most of these studies have overlooked the magnetic anisotropy between the rolling direction (RD) and the transverse direction (TD) since normally only the averaged magnetic properties measured on samples from both RD and TD are required according to standards for semi-processed NOES.[20] On the other hand, the magnetic properties were usually measured only at a frequency of 50 Hz or 60 Hz, which are not suitable for motors that work at higher frequencies.

In this study, the effect of the final annealing conditions such as temperature and time on the magnetic properties, magnetic anisotropy, and microstructure/texture of a low-silicon (0.5 wt.% Si) NOES was studied using commercially produced electrical steel sheets. Optimal final annealing conditions were determined by varying the annealing temperature and time. The magnetic property measurements were carried out using the Epstein frame method on strips cut along both the RD and TD. The measuring frequency was varied from 50–60 Hz up to 400 Hz and the magnetic flux density was varied from 0.5 T to 1.5 T. The relationships between the magnetic properties (core loss and relative magnetic permeability) and the frequency and magnetic flux density were established. Annealing experiments included both recovery and recrystallization (different annealing temperatures) so that the effect of stress releasing (recovery, without microstructure, and texture change) on the magnetic properties could also be investigated. The correlations between the magnetic properties and the microstructure, texture, and magnetocrystalline anisotropy energy were evaluated.

EXPERIMENTAL

The material investigated in this study was a commercially produced NOES containing 0.5% Si, 0.30% Al, and less than 0.003% C (all in weight percentages). The sheet thickness was 0.5 mm after cold rolling. After batch annealing (775°C for 24 h), it was further reduced to 0.47 mm (6% thickness reduction) by temper rolling (without tension). Epstein frame strips (28 cm × 3 cm) were cut from batch-annealed and temper-rolled sheets, and the magnetic properties were measured at a series of frequencies of 50 Hz, 60 Hz, 100 Hz, 200 Hz, and 400 Hz. Temper-rolled Epstein frame strips were annealed at different temperatures (500°C, 600°C, 700°C, 750°C, 775°C, 800°C, 825°C, 850°C, and 900°C) and times (0.5 h, 1.0 h, 2.0 h, 4.0 h, 12 h, and 24 h) in the laboratory using a tube furnace, and the magnetic properties were remeasured. During annealing, argon was injected into the tube to prevent oxidation. The furnace was first heated to the designated temperature and then the steel strips were quickly inserted into the furnace and held for the designated time. After reaching the annealing time, the furnace was turned off and the steel strips were cooled in the furnace (with argon flowing) to room temperature. The magnetic properties were measured on 8 steel strips consisting of all RD and all TD to evaluate the magnetic anisotropy, and a mix of 4 RD and 4 TD (standard measurement according to ASTM A726)[20] using a SMT-700 Epstein frame system (Magnetic Instrumentation, USA). The core losses and relative permeabilities at different flux density (B) levels, i.e., 0.5 T, 0.75 T, 1.0 T, 1.25 T, and 1.5 T, and various frequencies (50 Hz, 60 Hz, 100 Hz, 200 Hz, and 400 Hz) were recorded.

The microstructures and textures of selected samples (batch-annealed, temper-rolled, annealed at 600°C, 800°C, and 900°C for 2 h, and annealed at 800°C for 24 h) were characterized by electron backscatter diffraction (EBSD) techniques in a Nova

NanoSEM (FEI) scanning electron microscope (SEM) equipped with an EDAX OIM system (V8.1). EBSD samples were prepared using conventional metallographic procedures plus a final polishing step using a 0.05-μm colloidal silica suspension. The EBSD scans were performed on the RD–TD planes (at mid-thickness) of the sheets. The textures are represented by orientation distribution functions (ODFs) calculated from the EBSD orientation data using a harmonic series expansion method with a series rank of 22 and a Gaussian half-width of 5°. The ODFs were plotted on the $\varphi_2 = 45°$ section of the Euler space (Bunge notation). The magnetocrystalline anisotropy energy (MAE) was evaluated using the anisotropy factor[21] calculated in both the RD and TD from the ODFs, which was compared to the measured magnetic properties such as core loss and relative permeability to reveal the correlations between them.

RESULTS

Magnetic Properties After Annealing at Different Temperatures

The measured core losses at 1.5 T and 60 Hz for samples after different processing conditions are shown in Fig. 1. The core losses of the steel after batch annealing (before temper rolling) are 6.24, 6.53, and 6.34 W/kg for the RD, TD, and mixed samples, respectively (Fig. 1a). The core loss is about 5% lower in the RD than in the TD (Fig. 1b). After temper rolling, the core losses increase significantly to 9.50 (RD), 9.88 (TD), and 9.69 (mix) W/kg, respectively, with a 53% increase in the mixed samples. It is also noted that, after temper rolling, the core loss in the RD becomes about 4% higher than in the TD, due to a 58% increase in the RD and only a 45% increase in the TD. Apparently, temper rolling not only increases the overall core loss but also reverses the direction of anisotropy in core loss.

After annealing at 500°C for 2 h, the core losses were only slightly reduced but the difference (anisotropy) in core loss between the RD and the TD is significantly reduced to less than 0.4% (from 4% after temper rolling), and the core loss in the RD is now again lower than that in the TD. Increasing the annealing temperature to 600°C further reduces the core losses, and the difference in core loss between RD and TD increases to 1.6%. Further increasing the annealing temperature to 700°C continues to reduce the core losses, but at a smaller rate; the anisotropy in core loss further increases to 3.0%. After annealing at 750°C for 2 h, the core loss in the RD is reduced to 6.68 W/kg (from 6.84 W/kg), but that in the TD is increased to 7.36 W/kg (from 7.04 W/kg). As a result, the core loss in the mixed samples slightly increases. In this case, the anisotropy in core loss between the RD and the TD reaches 10% (Fig. 1b).

When the annealing temperature is increased to 775°C, the core losses in both the RD and TD are reduced, and the anisotropy between RD and TD is decreased to 7%. When the annealing temperature is raised to 800–825°C, the core losses are reduced to 5.6 (RD), 5.9–6.0 (TD), and 5.8 (mix) W/kg (the lowest), respectively; the anisotropy in core loss after annealing at 825°C is slightly higher (7.7%) than that after annealing at 800°C (5%). Further increasing the annealing temperature to 850°C or 900°C increases the core losses again, and the anisotropy in core loss is also increased. Thus, if the annealing time is fixed at 2 h, the optimal annealing temperature is 800–825°C and annealing at 800°C gives rise to a slightly lower anisotropy in core loss between the RD and TD.

The relative permeabilities of the steel measured at 1.5 T and 60 Hz are shown in Fig. 2. The relative permeabilities after batch annealing (before temper rolling) are not very high (1357–1500) (see Fig. 2a). There is a 10% difference between the RD and the

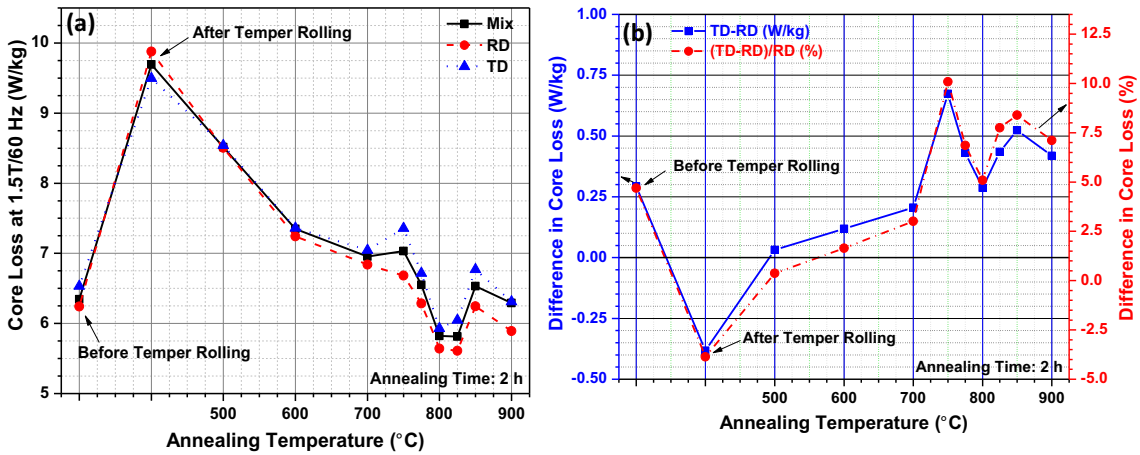

Fig. 1. The variation of core loss (1.5 T and 60 Hz) of the electrical steel with respect to the processing conditions: (a) core losses in the RD, TD, and mixed samples, (b) differences in core loss between the RD and TD samples: (TD–RD)/RD × 100%.

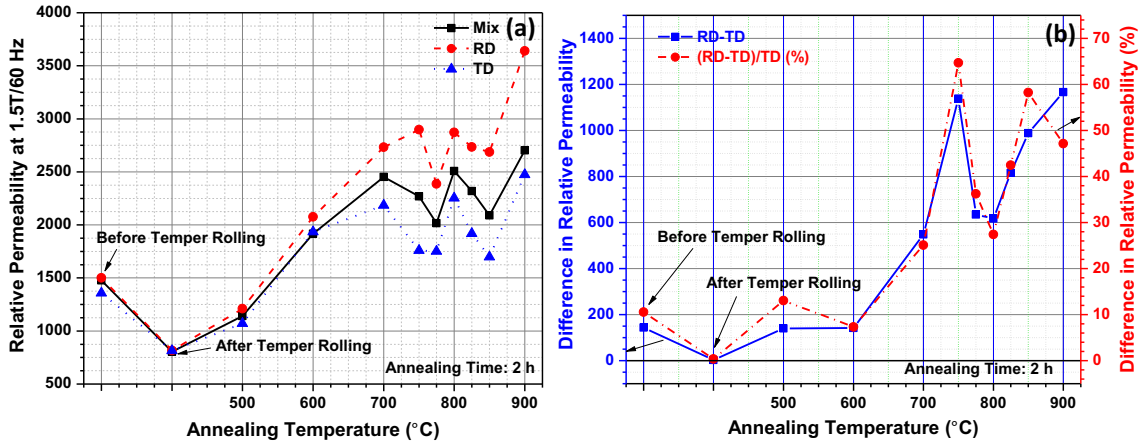

Fig. 2. The variation of relative permeability (1.5 T and 60 Hz) of the electrical steel with respect to the processing conditions: (a) relative permeabilities in the RD, TD, and mixed samples, (b) difference in relative permeability between the RD and TD samples: (RD–TD)/TD × 100%.

TD (Fig. 2b), with RD having a higher permeability than TD. Temper rolling not only significantly increases the core losses (as shown before) but also largely reduces the relative permeabilities of the electrical steel (40–46% reduction). It is noted that the anisotropy in relative permeability between the RD and the TD is essentially reduced to 0% after temper rolling. Annealing at increasing temperatures, e.g., 500°C, 600°C, and 700°C, gradually increases the relative permeabilities (to 2452 in the mixed samples) and the anisotropy in relative permeability (from 0% to 25%). When the annealing temperature is increased to 750°C and 775°C, the relative permeabilities drop again while the anisotropy significantly increases to 65% and 36%, respectively. When the annealing temperature is 800 °C, the relative permeability increases to 2508 in the mixed samples and the anisotropy is decreased to 27%. After annealing at 825°C and 850°C, the relative permeabilities drop again, and the anisotropy increases again. Annealing at 900°C gives rise to the highest relative permeabilities of 3640 (RD), 2474 (TD), and 2703 (mix), but at this temperature, the core losses are higher than those annealed at 800°C and 825°C, as shown before. Thus, the optimal annealing temperature for this steel after temper rolling is 800°C where the core losses are the lowest, the relative permeability is high, and the anisotropy in magnetic properties is small. Thus, the annealing temperature has been selected as 800°C for experiments with different annealing times.

Effect of Annealing Time on Magnetic Properties

When the annealing time is increased from 0.5 h to 4 h at a fixed annealing temperature of 800°C, the core loss (in the mixed samples) at 1.5 T and 60 Hz gradually decreases from 6.58 W/kg to 5.74 W/kg (a 13% reduction) (see Fig. 3a); however, the anisotropy in core loss increases from 5.8% to 12.2% (Fig. 3b). After annealing for 4 h, although the core loss in the mixed samples is slightly lower than that after annealing for 2 h, the core loss in the TD is higher than that after annealing for 2 h, indicating a large anisotropy between the RD and the TD. Further increasing the annealing time to 12 h and 24 h slightly increases the core losses. The smallest anisotropy in core loss (5%) is observed after annealing for 2 h. Thus, the optimal annealing time is 2 h when the annealing temperature is 800°C if the core loss is considered.

The relative permeability essentially shows an opposite trend to the core loss when the annealing time is gradually increased (Fig. 4a). The relative permeability in the mixed samples increases from 2476 to ~ 2903 (a 17% increase) when the annealing time is increased from 0.5 h to 12 h; after annealing for 24 h, the relative permeability drops to 2402. The smallest anisotropy (27%) in relative permeability is observed after annealing for 2 h, while the largest anisotropy (71%) is seen after annealing for 4 h. Considering both the core loss and relative permeability, 800°C for 2 h can be determined as the optimal annealing condition for the 0.5 wt.% Si steel after temper rolling.

Magnetic Properties at Different Magnetic Flux Densities

Non-oriented electrical steels may be utilized at different levels of magnetic induction depending on the application; thus, it is of interest to assess the magnetic properties of the steel at different magnetic flux densities. In addition, it is also of interest to examine the effect of residual stress on the magnetic properties at different magnetic inductions. Thus, the core loss and relative permeability of the samples after temper rolling and annealing at different temperatures have been plotted against the magnetic flux density. The Steinmetz equation states that the core loss is proportional to the power functions (with powers smaller than 3) of the peak

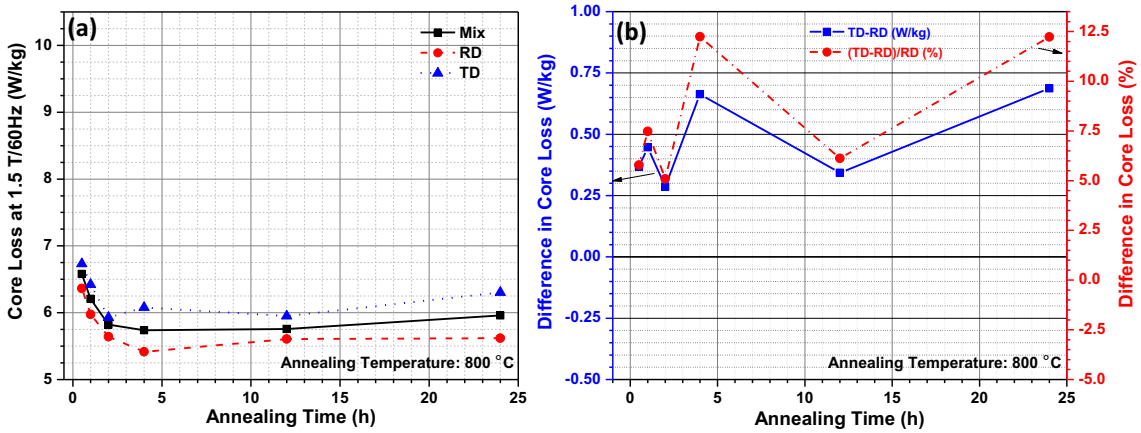

Fig. 3. The variation of core loss (1.5 T and 60 Hz) of the electrical steel with respect to the annealing time (at 800°C): (a) core losses in the RD, TD, and mixed samples, (b) difference in core loss between the RD and TD samples: (TD–RD)/RD × 100%.

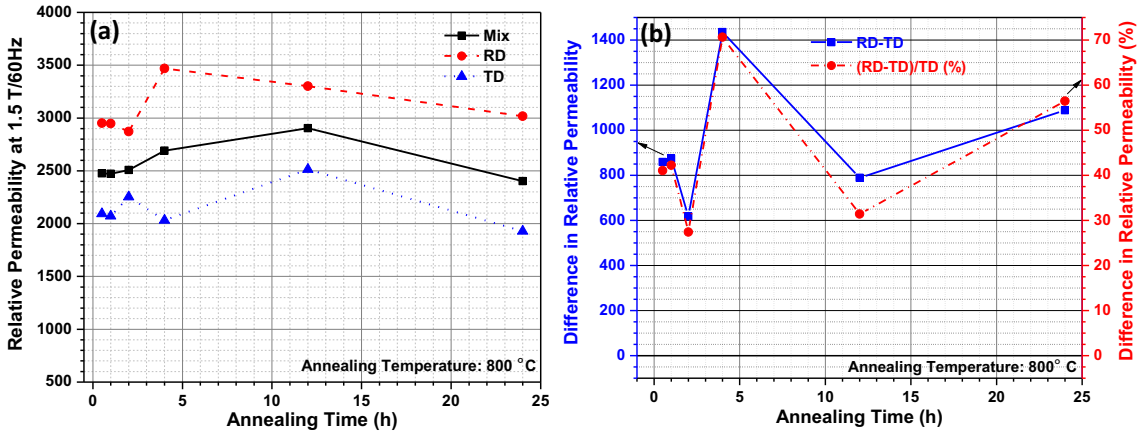

Fig. 4. The variation of relative permeability (1.5 T and 60 Hz) of the electrical steel with respect to the annealing time (at 800°C): (a) relative permeabilities in the RD, TD, and mixed samples, (b) difference in relative permeability between the RD and TD samples: (RD–TD)/TD × 100%.

magnetic flux density and frequency.[22,23] Thus, in this study, the core loss data is fitted using polynomial functions (with a maximum order of 2) when either the frequency or the magnetic flux density is fixed. Figure 5a shows the variation of the core losses of the mixed samples at different magnetic flux densities from 0.50 T to 1.5 T (at a fixed frequency of 60 Hz). It can be seen that the trends for all the samples are the same, and that they can all be almost perfectly fitted (with adjusted R^2 values greater than 0.99) using quadratic polynomial functions:

$$\boldsymbol{P} = c_0 + c_1\boldsymbol{B} + c_2\boldsymbol{B}^2 \qquad (1)$$

where c_0, c_1, and c_2 are the coefficients of the polynomial. This relationship holds for all the samples no matter if the material is plastically deformed (after temper rolling), recovered, or recrystallized. The anisotropy in core loss, on the other hand, is highly dependent on the state of the steel (Fig. 5b). If the steel is temper-rolled or the annealing temperature is low (500–700°C), the core loss in the RD is normally higher than that in the TD, especially when the magnetic induction level is low (0.5–1.25 T). The largest difference in core loss between the TD and the RD is 18% when the steel is temper-rolled at a magnetic flux density of 0.5 T. With the increase of the annealing temperature, the anisotropy gradually decreases. When the annealing temperature is at or higher than 750°C, the anisotropy in core loss changes its direction, i.e., the core loss in the RD becomes smaller than that in the TD at all magnetic flux densities. The largest anisotropy in core loss between the RD and the TD is 10% when the steel is annealed at 750°C for 2 h (B = 1.5 T). Apparently, the release of the residual stress in the material and the change of the microstructure and texture by annealing not only reduces the overall core loss but also reduces the anisotropy and changes its direction.

While the prediction of core loss using empirical equations has been extensively studied, investigations on the dependence of magnetic permeability

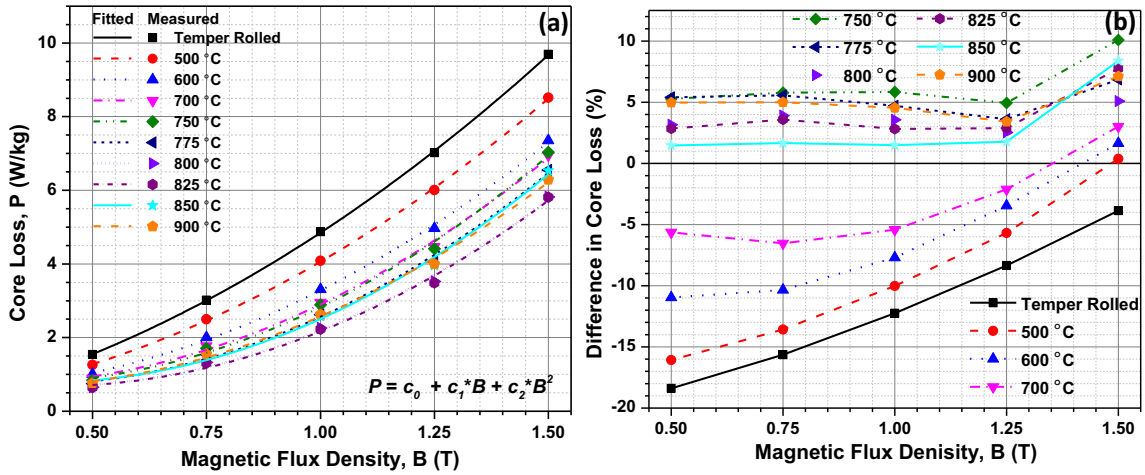

Fig. 5. The variation of core loss with respect to the magnetic flux density at 60 Hz for samples after temper rolling and annealing at different temperatures: (a) core losses of the mixed samples, (b) difference in core loss between the RD and TD: (TD–RD)/RD × 100%.

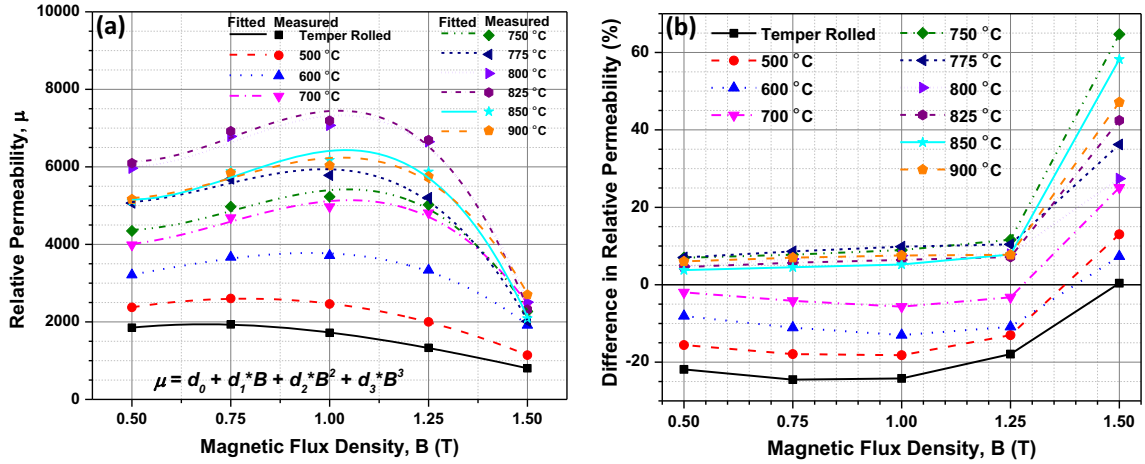

Fig. 6. The variation of relative permeability with respect to the magnetic flux density at 60 Hz for samples after temper rolling and annealing at different temperatures: (a) relative permeabilities of the mixed samples, (b) difference in relative permeability between the RD and TD: (RD–TD)/TD × 100%.

on magnetic flux density and frequency are rarely seen in the literature. The magnetic permeability itself is nonlinear to the magnetic field and is assumed to mainly depend on the material. However, it has been found in this study that, within the examined magnetic flux density levels (0.5–1.5 T) and frequencies (50–400 Hz), the relative magnetic permeability shows clear dependence on both the magnetic flux density (when the frequency is fixed) and the frequency (when the magnetic flux density is fixed). The variation of the relative permeability (mixed samples) with respect to the magnetic flux density is shown in Fig. 6. The relative permeabilities follow cubic polynomial functions with respect to the magnetic flux density (adjusted R^2 values range from 0.96 to 1), again, no matter if the material is deformed, recovered, or recrystallized:

$$\mu = d_0 + d_1 B + d_2 B^2 + d_3 B^3 \quad (2)$$

Where d_0, d_1, d_2, and d_3 are coefficients of the polynomial. Increasing the annealing temperature gradually increases the relative permeability at all the magnetic flux densities until the temperature reaches 800–825°C at which the highest relative permeabilities are achieved for all magnetic induction levels except 1.5 T (where annealing at 900°C achieves the highest relative permeability). Further increasing the annealing temperature generally decreases the relative permeability. For all the samples except those after temper rolling and annealing at 500°C, the maximum relative permeability is observed at a magnetic induction of 1.0 T. When the magnetic induction reaches 1.5 T, the relative permeability significantly reduces, with the

lowest occurring in the plastically deformed samples.

The anisotropy in relative permeability also changes direction when the temper-rolled steel is annealed. When the steel is deformed or annealed at relatively low temperatures (up to 700 °C), the relative permeabilities in the TD are larger than those in the RD at low magnetic flux densities (0.5–1.25 T), with the largest difference (24.5%) at 0.75 T for the temper-rolled steel. Increasing the annealing temperature generally decreases the anisotropy; when the annealing temperature is 750°C or higher, the anisotropy changes direction, i.e., the relative permeability in the RD becomes larger than that in the TD. At 1.5 T, all the samples show larger relative permeabilities in the RD than those in the TD and the anisotropy in relative permeability reaches 65% when the annealing temperature is 750°C. It is also noted that the anisotropy in relative permeability for samples annealed at temperatures of 750°C or above is relatively small (below 12%) if the magnetic induction is between 0.5 T and 1.25 T; when the magnetic induction increases to 1.5 T, the anisotropy increases to more than 27%.

Magnetic Properties at Different Magnetization Frequencies

The core losses of the electrical steel measured at 50 Hz, 100 Hz, 200 Hz, and 400 Hz are illustrated in Fig. 7. The data for all the samples can be perfectly fitted (adjusted $R^2 = 1$) using quadratic polynomial functions at both high (B = 1.5 T) and low (B = 1.0 T) magnetic inductions:

$$\boldsymbol{P} = k_0 + k_1\boldsymbol{f} + k_2\boldsymbol{f}^2 \tag{3}$$

Again, this is independent of the state of the steel (deformed, recovered, or recrystallized). Although the plastic deformation increases the core loss, it does not change the correlation between the core loss and the frequency. Annealing at different temperatures reduces the core loss, but it also does not alter the correlation. When the magnetic induction is low (B = 1.0 T), the discrepancies in core loss between the deformed and annealed samples

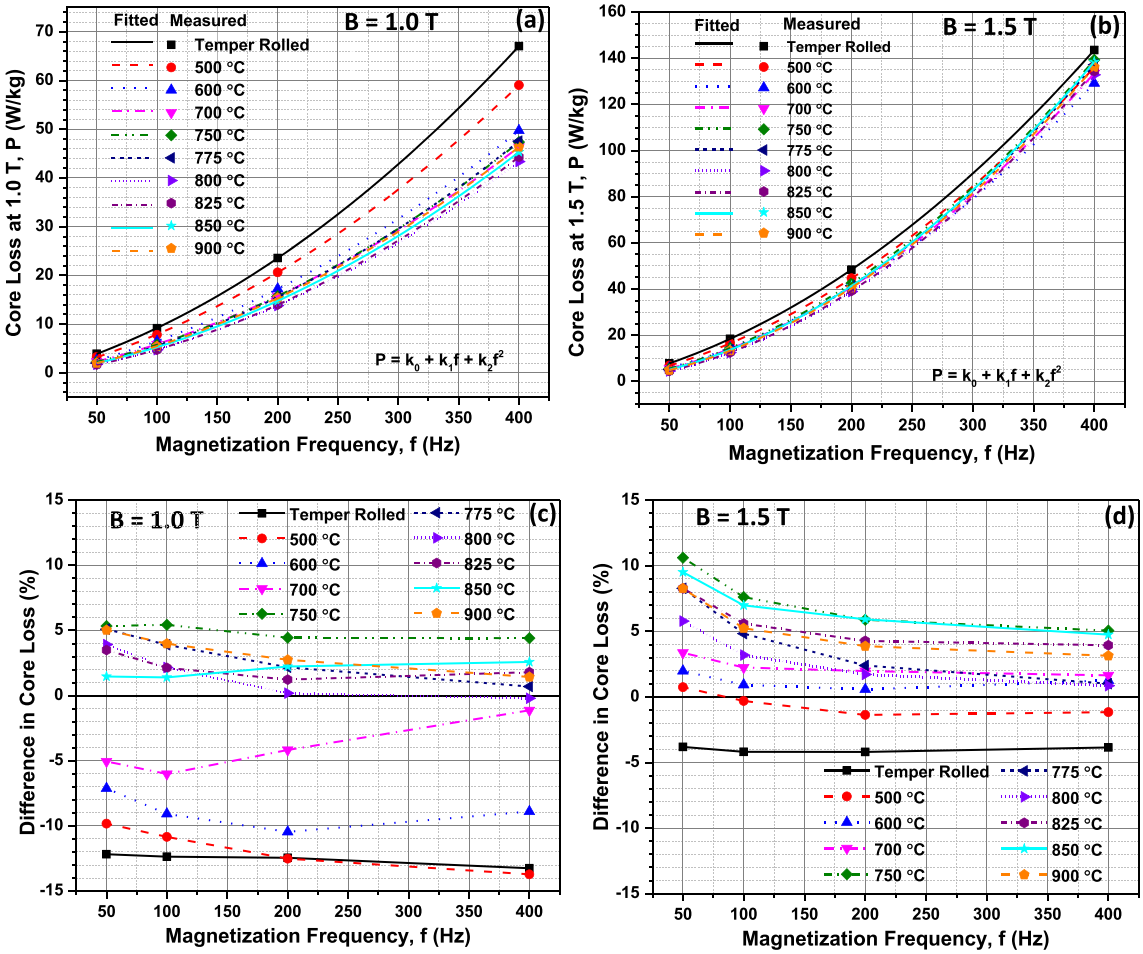

Fig. 7. Variation of the core loss with respect to the magnetization frequency for samples after temper rolling and annealing at different temperatures: (a) core losses at B = 1.0 T, (b) core losses at B = 1.5 T, (c) difference in core loss at B = 1.0 T, (d) difference in core loss at B = 1.5 T. The difference in core loss is calculated as: (TD–RD)/RD × 100%.

increase significantly from 2.2 W/kg to 23.7 W/kg with the increase of frequency from 50 Hz to 400 Hz (Fig. 7a). If the magnetic induction is high (B = 1.5 T), the discrepancies also increase with frequency, but at a much smaller rate, i.e., from 3.3 W/kg to 14.4 W/kg (Fig. 7b). This means that the effect of plastic deformation on the core loss is reduced if the frequency and magnetic flux densities are high.

The anisotropy in core loss is affected by the magnetization frequency, magnetic flux density, and the material state. When the magnetic flux density is low (B = 1.0 T), plastic deformation (temper rolling) causes large differences between the RD and TD (up to 13%); the core losses in the RD are larger than those in the TD. However, the anisotropy is essentially not affected by the frequency (Fig. 7c). Annealing generally decreases the anisotropy and, when the annealing temperature is higher than 700°C, the direction of the anisotropy is changed, i.e., the core losses in the RD are smaller than in the TD. The maximum anisotropy is reduced to below about 5% at all frequencies. When the magnetic induction is high (B = 1.5 T), the anisotropy caused by the plastic deformation (temper rolling) is much smaller than at low inductions, i.e., smaller than 5% (Fig. 7d). Again, the anisotropy is essentially not affected by the frequency. Annealing reduces the anisotropy at all frequencies and changes the anisotropy direction; at a relatively low annealing temperature of 600°C, the anisotropy direction is changed for all frequencies. The anisotropy generally decreases with increasing frequency. At 50 Hz, the maximum anisotropy reaches more than 10%, while at 400 Hz, the maximum anisotropy is less than 5%.

The correlation between the relative permeability and the magnetization frequency is shown in Fig. 8. In all the cases, the relative permeability can be perfectly fitted (adjusted R^2 = 1) using cubic polynomial functions with respect to the frequency:

$$\boldsymbol{\mu} = h_0 + h_1\boldsymbol{f} + h_2\boldsymbol{f}^2 + h_3\boldsymbol{f}^3 \qquad (4)$$

Generally, with increasing frequency, the relative permeability decreases at both high (B = 1.5 T) and low (B = 1.0 T) magnetic flux densities for almost all the samples. The only exception is that, when the magnetic flux density is 1.5 T, the relative permeabilities of the temper-rolled sample and the sample annealed at 500°C slight increase when the frequency is increased from 50 Hz to 100 Hz. At a low magnetic flux density of 1.0 T, the samples annealed at 800°C and 825°C show the highest relative permeability at all frequencies, while at 1.5 T, the sample annealed at 900°C shows the highest relative permeability at all frequencies. At 1.0 T, the largest discrepancy in relative permeability between the deformed and annealed samples is 5941 when the frequency is 50 Hz and is significantly reduced to 1270 when the frequency is 400 Hz (Fig. 8a). At 1.50 T, the discrepancies in relative permeability between the deformed and annealed samples are much smaller, 1906 at 50 Hz and 820 at 400 Hz. This means that, at higher magnetic flux densities, the decrease of relative permeability caused by deformation is largely reduced.

Microstructure and Crystallographic Texture

The microstructure and texture of the steel after batch annealing and temper rolling are shown in Fig. 9. After batch annealing at 775°C for 24 h (Fig. 9a), the steel is composed of non-uniformly distributed grains with diameters ranging from about 3 μm to more than 260 μm (average grain size $\sim$ 82 μm). The texture (Fig. 9c) is quite different from the typical texture of electrical steel after cold rolling and annealing, i.e., there is no continuous α-fiber (<110> //RD) or γ-fiber (<111> //ND), although a rotated cube ({001} <110>) and a {111} <110> are noticed. There are two components, {112} <285> and {110} <112> (brass), that are rarely seen in electrical steels after cold rolling and annealing. This might be caused by the industrial batch annealing process which is different from continuous annealing or laboratory-scale annealing usually reported in the literature. Nevertheless, these unconventional textures need to be confirmed using other methods, e.g., X-ray diffraction, on statistically large number of grains, since the textures measured by EBSD in this study only covered a small number of grains. After temper rolling (with 6% thickness reduction), the microstructure and texture are only slightly changed (Fig. 9b and d). The average grain size is slightly decreased to $\sim$ 80 μm, and the major textures are still the {112} <285> and {110} <112>. The rotated cube ({001} <110>) is slightly shifted to {115} <110>, and the {111} <110> is slightly moved to {553} <110>.

The microstructure and texture of samples after annealing at different temperatures for 2 h are shown in Fig. 10. Annealing of the temper-rolled steel at a relatively low temperature (600°C, 2 h) only slightly increases the average grain size, from $\sim$ 80 μm (Fig. 9b) to $\sim$ 85 μm (Fig. 10a). The main features of the texture essentially do not change (Figs. 9d and 10c), i.e., the {112} <285> and {110} <112> orientations remain as the main textures, although the {001} <110>, {115} <110> and {553} <110> components are weakened, which indicates that very little recrystallization has occurred. If the annealing temperature is increased to 800°C (2 h), not only is the grain size significantly increased to 165 μm (Fig. 10b) but the texture is also remarkably changed (Fig. 10d). The texture is randomized (with the maximum intensity reduced to 2.7) and the main components now include {221} <598>, {110} <100> and {111} <110>. Other

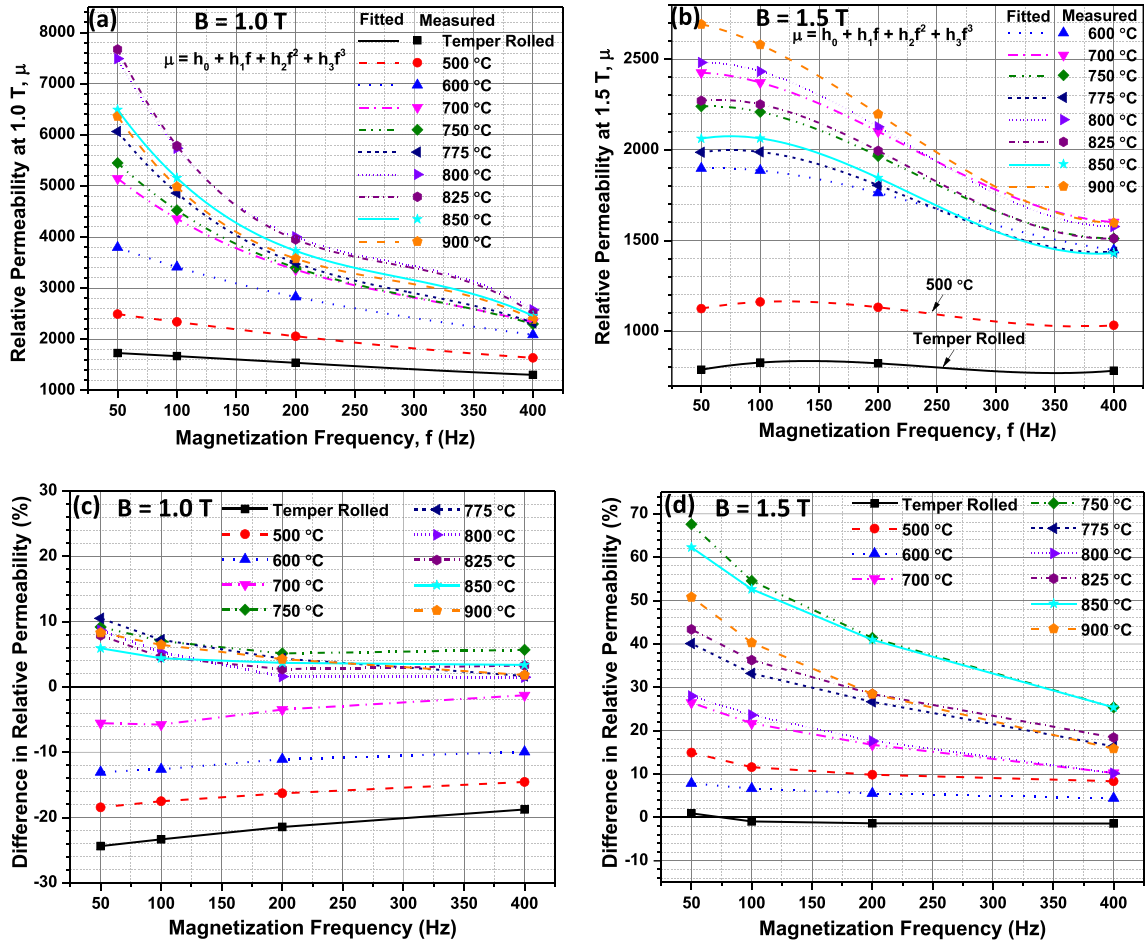

Fig. 8. Variation of the relative permeability with respect to the magnetization frequency for samples after temper rolling and annealing at different temperatures: (a) relative permeabilities at $B = 1.0$ T, (b) relative permeabilities at $B = 1.5$ T, (c) difference in relative permeability at $B = 1.0$ T, (d) difference in relative permeability at $B = 1.5$ T. The difference in relative permeability is calculated as: (RD–TD)/TD × 100%.

components such as {001} <140>, {115} <110> and {112} <576> are also noticed.

If the annealing temperature is kept at 800°C, but the annealing time is increased to 24 h, the grain size is only moderately increased from 165 μm to 195 μm (Fig. 11a). However, the texture has changed significantly, i.e., a <001> //ND fiber (without the cube though) is formed while the γ-fiber components are mostly eliminated (Fig. 11c). The intensity of the texture is again significantly reduced. Some uncommon components such as {331} <783>, {112} <132>, and {114} <221> are also noticed. If the annealing time is fixed at 2 h but the annealing temperature is increased to 900°C (Fig. 11b), a significant increase in grain size is noticed (from 165 to 347 μm). The texture is also changed, i.e., the <001> //ND fiber is mostly eliminated (Fig. 11d). Again, some uncommon components such as {225} <232> and {332} <596> are seen in the texture. However, it should be noted that the grain size of this sample is very large, so the number of grains covered by the EBSD scan is small. Thus, the texture may not be statistically representative.

DISCUSSION

The magnetization process in ferromagnetic materials (e.g., electrical steels) mainly takes place through the movements of magnetic domain walls, which are discontinuous in nature and give rise to the magnetic Barkhausen noise.[24,25] The composition, microstructure, stress configuration, crystallographic texture, etc. all affect the magnetic domain configurations and domain wall movements, thus influencing the magnetization process and the magnetic properties. The magnetization loss, i.e., the damping of the domain wall motion by eddy currents,[23,26–28] is highly dependent on the microstructure, texture as well as the stress state of the material.

It has been shown in this study that even a 6% thickness reduction during temper rolling significantly increases the core loss by more than 50%.

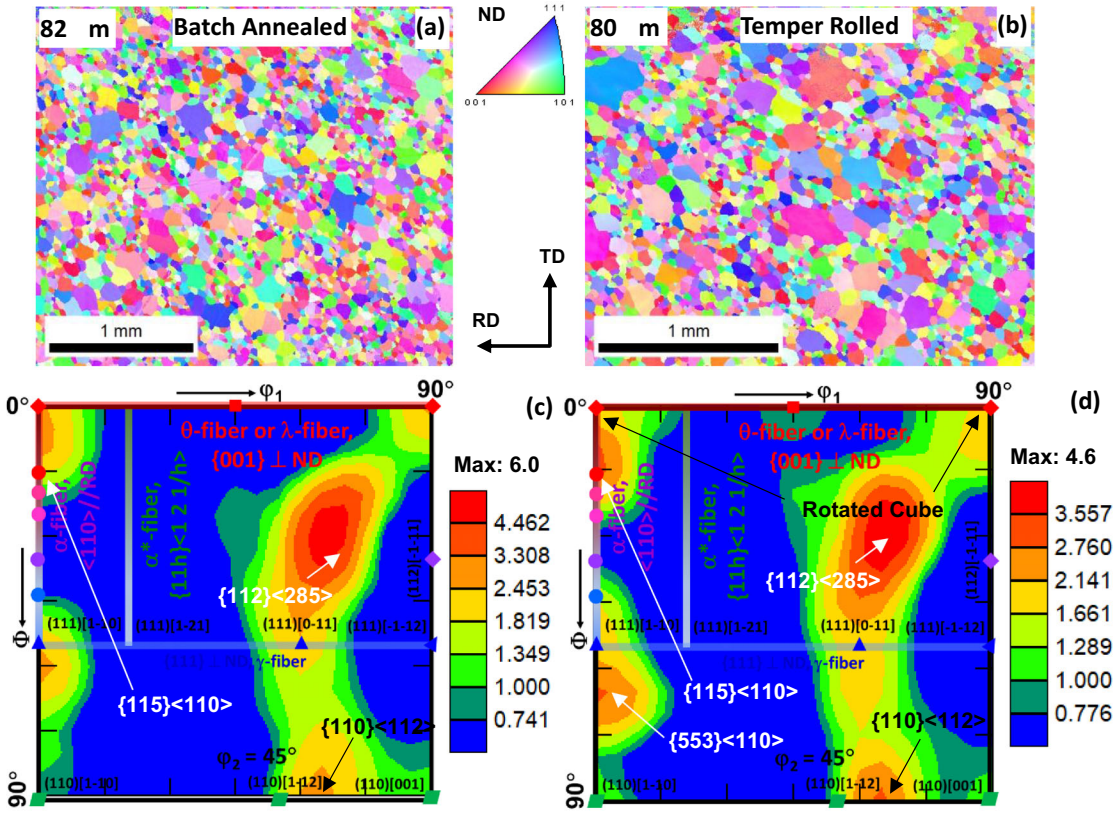

Fig. 9. Microstructure and crystallographic texture of the steel after batch annealing and temper rolling: (a and b) EBSD inverse pole figure (IPF) maps of batch-annealed and temper-rolled samples, respectively, (c) and (d) textures of the batch-annealed and temper-rolled samples, respectively.

This is mainly caused by the dislocations created during plastic deformation. The slip during plastic deformation increases the number of dislocations (dislocation density) in the material. Near the dislocations, strain fields are generated, which contribute to the redistribution of strain within grains and change the volume of the magnetic domains. The created strain fields increase the number of magnetic domains,[25] leading to the increase of domain walls. Dislocation pileups and tangles also act as pinning sites to domain wall movement. As a result, the core loss increases since larger resistance must be overcome during magnetization. After rolling, residual stresses (elastic in nature) will remain in the deformed material, which increases the wall energy gradient and the magnetic field required to move domain walls,[25,29] also leading to higher core loss.

Annealing at a relatively low temperature (e.g., 500°C) does not cause obvious change of the microstructure since only recovery (no recrystallization) has occurred in the material. However, recovery reduces the dislocation density and changes the dislocation structure through dislocation annihilation and rearrangement, which reduces the number of magnetic domains and the number of pinning sites, leading to the decrease of the core loss. Recovery also partially releases the residual stress, which also decreases the core loss. When the annealing temperature is increased to 600°C or above, recrystallization occurs in the microstructure, which not only alters the microstructure (as evidenced by the increase of the average grain size) and releases the residual stress but also changes the crystallographic texture (as evidenced by the increase in maximum texture intensity), leading to a further decrease of the core loss. Increasing the annealing temperature to 700°C or higher significantly changes the microstructure (much larger grain size) and crystallographic texture (very different textures), which changes the core loss. After recrystallization, the (macroscopic) residual stress is assumed to be completely released and the core loss is mainly determined by the microstructure and texture. As a result, the core loss does not any more decrease linearly with the increase of the annealing temperature. Similarly, changing the annealing time at a fixed temperature that is high enough to cause recrystallization will also result in different microstructures and textures, again leading to different magnetic properties.

The variation of the relative permeability with respect to the steel processing state is mainly caused by the changes in residual stress and texture. The large residual stresses in the steel

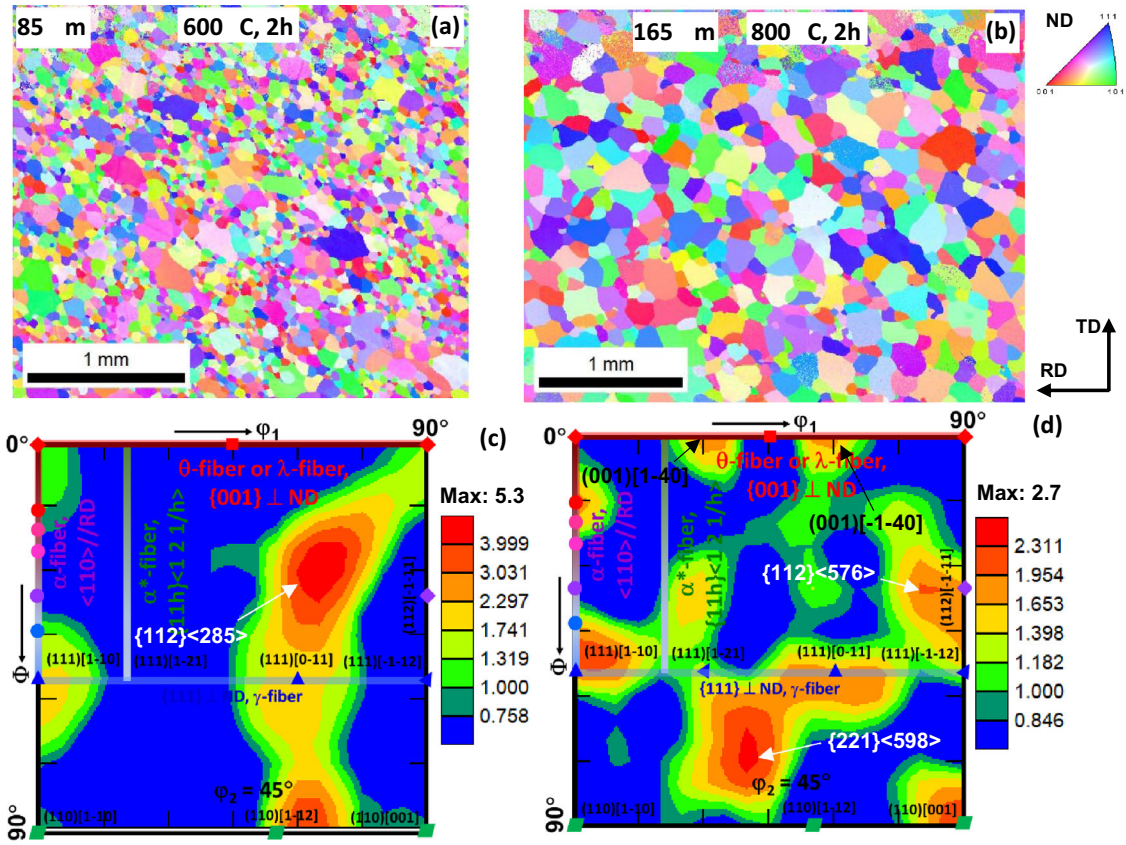

Fig. 10. Microstructure and crystallographic texture of the steel after temper rolling and annealing: (a) and (b) EBSD inverse pole figure (IPF) maps of samples after annealing at 600 and800°C, respectively, (c) and (d) textures of the samples after annealing at 600 and 800°C,[19] respectively.

after temper rolling cause a large decrease in relative permeability since the equivalent magnetic field due to stress (H_σ) is proportional to the stress (σ) according to Jiles and Atherton's theory:[30–32]

$$H_\sigma = \frac{3}{2}\frac{\sigma}{\mu_0}\frac{\mathrm{d}\lambda}{\mathrm{dM}} \tag{5}$$

where λ is the bulk magnetostriction, M is the magnetization, and μ_0 is the permeability of free space. The measured permeability at a given B ($\mu = B/H$) thus decreases with the increase of the residual stress in the material. Annealing releases the residual stress, therefore increasing the relative permeability. However, annealing at a relatively low temperature (where only recovery occurs), e.g., at 500°C, cannot completely release the residual stress or change the microstructure; thus, the relative permeability is lower than those after recrystallization. Once the (macroscopic) residual stress has been completely removed (annealing at 700°C or above), the determining factor of the relative permeability is assumed to be the crystallographic texture (magnetocrystalline anisotropy energy); the relative permeability shows significant variations since the texture and microstructure generated at these annealing temperatures are significantly different. It is also noted that, after the steel is recrystallized, the anisotropy in relative permeability between the RD and the TD increases significantly (Fig. 2).

The anisotropy of ferromagnetic materials mainly comes from two sources: the magnetocrystalline anisotropy (orientation dependence) and the magnetoelastic anisotropy (strain dependence).[33,34] The reverse of the anisotropy direction in core loss after temper rolling, i.e., the core loss in the TD becomes smaller than that in the RD, may be attributed to (1) residual stresses and dislocations that alter the magnetic domain configurations, (2) the formation of crystallographic texture that changes the magnetization easy axis, and (3) the microstructural inhomogeneities induced during plastic deformation that change the magnetic domain configurations. All of them affect the domain wall dynamics and contribute to magnetic anisotropy. Under stress, the direction of domain magnetization is determined by both the MAE and the magnetoelastic energy.

The MAE is determined by the crystallographic texture of the material, which can be calculated using the angles (α, β, γ) between the magnetization vector (**H**) and the crystal easy axes ($<001>$ for bcc iron). Two parameters have been frequently used to

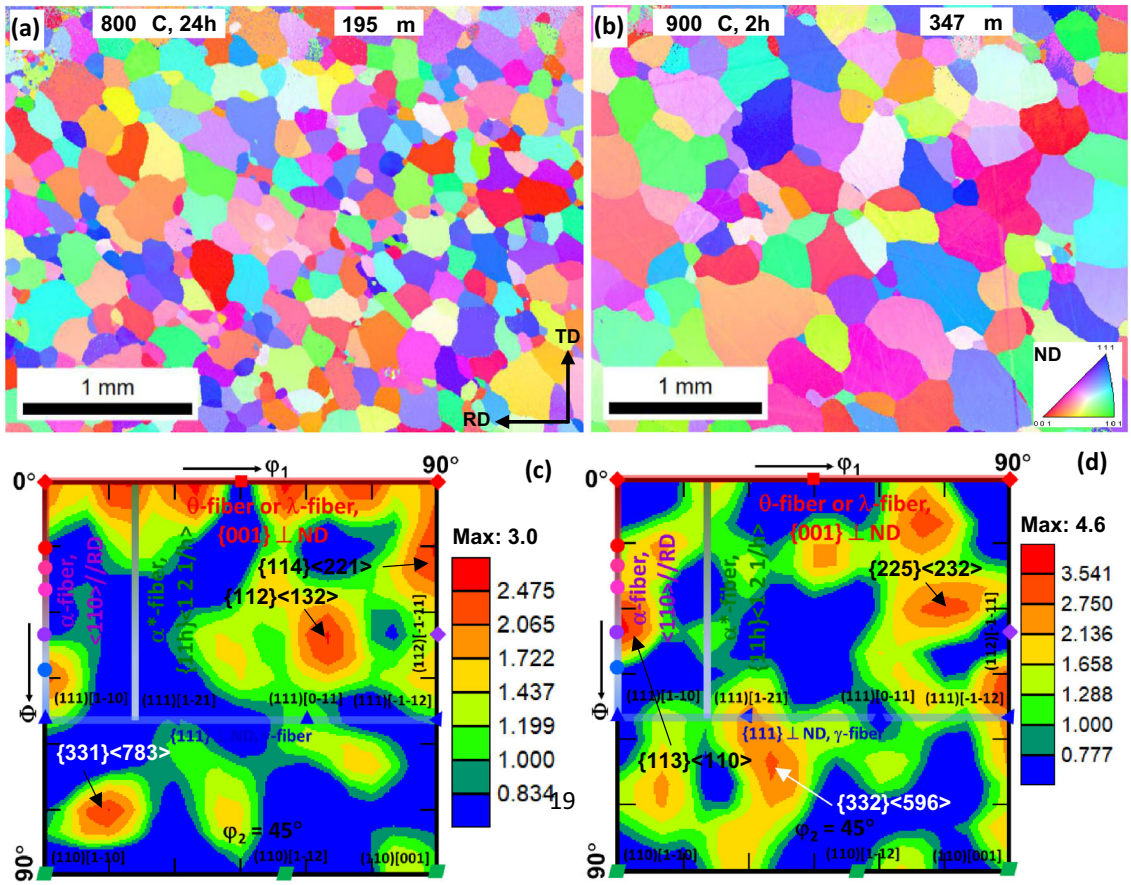

Fig. 11. Microstructure and crystallographic texture of the steel after temper rolling and annealing at 800°C for 24 h[19] and at 900°C for 2 h, respectively: (a) and (b) IPF maps, (c) and (d) textures.

characterize the magnetic quality of the texture, i.e., the texture factor,[3] A_θ, and the anisotropy factor,[21] $A(\vec{h})$:

$$A_\theta = \int f(g)\min(\alpha,\beta,\gamma)dg, A_\theta \in [0^\circ, 54.7^\circ] \quad (6)$$

$$A\left(\vec{h}\right) = \cos^2\alpha\,\cos^2\beta + \cos^2\gamma\,\cos^2\beta + \cos^2\alpha\,\cos^2\gamma,$$
$$A\left(\vec{h}\right) \in [0, 0.333] \quad (7)$$

The texture factor directly evaluates the average minimum angle between the magnetization vector and the easy axes of all the crystals in the material. Apparently, the smaller the texture factor, the closer the magnetization vector to the easy axes, and the better the magnetic quality. The anisotropy factor is directly related to the MAE as:[21,33]

$$E_{MAE} = K_1 A\left(\vec{h}\right) + K_2\left(\cos^2\alpha\,\cos^2\beta\cos^2\gamma\right) \quad (8)$$

where K_1 and K_2 are the anisotropy constants. Apparently, the smaller the anisotropy factor, the smaller the MAE. Using the orientation data (and the calculated ODFs) from the EBSD scans, the anisotropy factor can be calculated using Eq. 7. The results are then compared to the measured core loss and relative permeability, as shown in Fig. 12 (for annealed samples only).

For ferromagnetic materials with a positive magnetostriction (e.g., electrical steel), a tensile stress (in the elastic region) tends to align the magnetic domains (the easy magnetization axis) along the stress direction and enhances magnetic properties in the stress direction, while a compressive stress tends to align the domains perpendicular to the stress direction and thus disfavors the magnetization in the stress direction.[25,35–37] However, plastic stress induces much more complicated changes to the magnetic domain configuration, microstructure, and texture, which significantly affect the magnetic properties, but are very difficult to model. The residual stresses after plastic deformation also affect the magnetic properties. The change of the anisotropy direction in core loss after temper rolling may be attributed to the residual stresses in the steel (which are not accounted for in the anisotropy

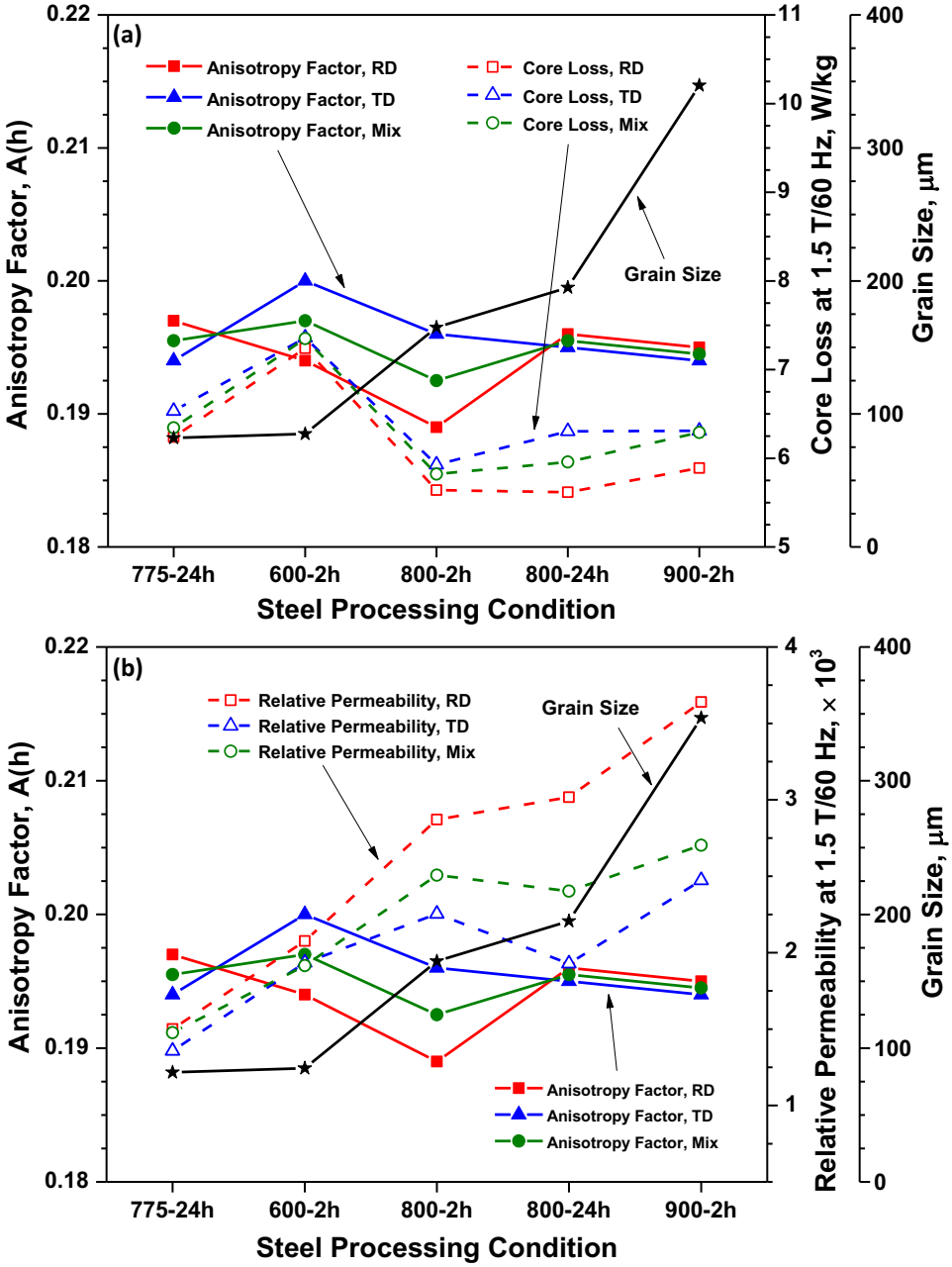

Fig. 12. The relationships between the magnetic properties and the anisotropy factor and average grain size: (a) core loss and (b) relative permeability at 60 Hz and 1.5 T. Note that annealing at 775°C for 24 h is after cold rolling, while all the other annealing is after temper rolling.

factor calculations), since the anisotropy factor caused by the texture is almost identical in the RD and the TD (0.196 and 0.200, respectively), while the anisotropy in core loss is not zero.

For annealed samples (Fig. 12), when the grain size is smaller than about 200 μm, the core loss generally follows a similar trend to the anisotropy factor, i.e., the smaller the anisotropy factor, the smaller the core loss. However, if the grain size is very large (347 μm), the core loss is increased although the anisotropy factor is decreased. As mentioned before, due to the large grain size, the texture (and thus the anisotropy factor) of this sample may not be statistically representative, which may have caused the deviation from the general trend. On the other hand, the difference in core loss between the RD and the TD is not reflected in the difference in anisotropy factor between the RD and the TD since the difference in core loss is always negative (core loss in the RD is lower than in

the TD), while the difference in anisotropy is not always negative (only annealing at 600°C for 2 h and 800°C for 2 h gives rise to lower anisotropy factors in the RD than in the TD).

The relative permeability generally follows a similar trend to the grain size but does not follow the trend of the anisotropy factor (Fig. 12b). However, when the grain size is 165 μm (annealing at 800°C for 2 h) or larger, a smaller (mixed) anisotropy factor normally corresponds to a larger (mixed) relative permeability. The difference in relative permeability between the RD and the TD is also not reflected in the difference in anisotropy factor. In all the cases, the relative permeability in the RD is higher than that in the TD, but the anisotropy factor in RD is smaller than that in TD only when the annealing is at 600°C for 2 h and at 800°C for 2 h. These discrepancies may be caused by the micro-scale residual stresses[38] which are present in the recrystallized materials,[39] but are not considered either in the MAE or the magnetoelastic energy (recrystallization is assumed to completely release the residual stress).

It is well known that the core loss of electrical steel is also closely related to the grain size. Hysteresis loss decreases with the grain size while eddy current and excess losses increase with the grain size.[40,41] As a result, there is an optimal grain size at which the total core loss is the lowest, which has been observed to be $\sim$ 165 μm (close to the 150 μm found in Ref. 41) for the NOES in this study (Fig. 12a). Annealing at 800°C for 2 h after temper rolling gives rise to the lowest anisotropy factors and an optimal grain size, leading to the lowest core losses.

The relationships between the core loss and the magnetic flux density (B) and frequency (f) as observed in this study may be explained by the "Best Fit" model frequently cited in the literature. The total core loss (P) is composed of three components, i.e., the hysteresis loss (P_h), the classical eddy current loss (P_{cl}), and the excess (anomalous) loss (P_e), and can be modeled as:[26,42]

$$P = P_h + P_{cl} + P_e = k_h B_m^{\alpha} f + k_{cl} B_m^2 f^2 + k_e B_m^{\frac{3}{2}} f^{\frac{3}{2}} \quad (9)$$

where k_h, k_{cl}, and k_e are the coefficients for hysteresis, classical eddy current, and excess loss components, respectively, B_m is the peak flux density, and α is the exponent of the flux density (α = 1.6–1.8 for NOES).[43,44] It should be noted that these coefficients do not possess physical meaning. It is seen that all three loss terms are related to the magnetic flux density, B, and the frequency, f. The correlation between the core loss and the magnetic flux density (when the frequency is fixed) as observed in this study, i.e., a quadratic polynomial function, agrees with the above relationship since the maximum power on the flux density is also 2. It has been shown that this relationship does not change even if the material is under different processing states, i.e., deformed, recovered, or recrystallized. Similarly, if the magnetic flux density is fixed, the relationship between the core loss and the frequency can also be modeled as a quadratic polynomial function, which again agrees with the above equation since the maximum power on the frequency is 2. Similarly, the processing state of the material does not affect the correlation function although the coefficients are different under different conditions.

The relationships between the relative permeability and the magnetic flux density and frequency in NOES have rarely been reported in the literature. The results from this study show that, when the frequency is fixed, the relative permeability first slightly increases with the flux density as a cubic polynomial function when the flux density is low; it then rapidly drops when the flux density is high. When the flux density is fixed, the relative permeability generally decreases with the frequency also according to a cubic polynomial function. It is noted that these functions apply to all the samples regardless of the processing states, i.e., deformed, recovered, or recrystallized. Again, the coefficients of these polynomials do not possess physical meaning. However, these functions are simple to use for the evaluation of magnetic properties of the electrical steel under different magnetization conditions.

CONCLUSION

A semi-processed, low-silicon non-oriented electrical steel was temper-rolled and annealed at different temperatures (with a fixed time of 2 h) and times (with a fixed temperature of 800°C). The magnetic properties in both the RD and the TD were measured using the Epstein frame method, and the anisotropies in both core loss and relative permeability were evaluated, which were compared to the grain size and anisotropy factor obtained from microstructure and texture analysis. The findings are summarized as follows:

(1) The optimal annealing condition for the temper-rolled steel was found to be 800–825°C for 2–4 h, which give rise to the lowest core loss, very high relative permeability, and small anisotropy in both core loss and relative permeability.

(2) Temper rolling not only increases the core loss and reduces the relative permeability, but also reverses the anisotropy direction in core loss, i.e., makes the core loss higher in RD than in the TD, which is opposite to that after annealing; temper rolling reduces the anisotropy in relative permeability between the RD and the TD to almost 0.

(3) The core loss follows quadratic polynomial functions with respect to both the magnetic flux density (when the frequency is fixed) and frequency (when the magnetic flux density is fixed); this relationship applies to the NOES

regardless of the processing state, i.e., deformed, recovered, or recrystallized.

(4) The relative permeability follows cubic polynomial functions with respect to both the magnetic flux density (when the frequency is fixed) and frequency (when the magnetic flux density is fixed), again regardless of the processing state of the material.

(5) The core loss generally follows a similar trend to the anisotropy factor, i.e., a higher anisotropy factor leads to a higher core loss, while the relative permeability generally does not correspond to the anisotropy factor; the optimal grain size (where the lowest core loss is obtained) is 165 μm, which is obtained after annealing at 800°C for 2 h.

(6) The anisotropy in magnetic properties (core loss and relative permeability) between the RD and the TD cannot be accounted for by the anisotropy factors calculated in these directions from the texture data, even after the material has been fully recrystallized (macro-scale residual stresses have been released); micro-scale residual stress in the material might have played a role in determining the anisotropy.

ACKNOWLEDGEMENTS

Funding for this research was provided by the Program of Energy Research and Development (PERD), Natural Resources Canada. The authors are grateful to Michael Attard and Mehdi Mehdi for their help on annealing the steel strips. Jian Li and Renata Zavadil are gratefully acknowledged for the EBSD measurements.

FUNDING

Open Access funding provided by Natural Resources Canada.

CONFLICT OF INTEREST

The authors declare that they have no conflict of interest.

OPEN ACCESS

This article is licensed under a Creative Commons Attribution 4.0 International License, which permits use, sharing, adaptation, distribution and reproduction in any medium or format, as long as you give appropriate credit to the original author(s) and the source, provide a link to the Creative Commons licence, and indicate if changes were made. The images or other third party material in this article are included in the article's Creative Commons licence, unless indicated otherwise in a credit line to the material. If material is not included in the article's Creative Commons licence and your intended use is not permitted by statutory regulation or exceeds the permitted use, you will need to obtain permission directly from the copyright holder. To view a copy of this licence, visit http://creativecommons.org/licenses/by/4.0/.

REFERENCES

1. D. Steinberg, D. Bielen, J. Eichman, K. Eurek, J. Logan, T. Mai, C. McMillan, A. Parker, L. Vimmerstedt, and E. Wilson, National Renewable Energy Laboratory, Technical Report, NREL/TP-6A20-68214, pp. 1-53, 2017.
2. N.L. Panwar, S.C. Kaushik, and S. Kothari, *Renew. Sustain. Energy Rev.* 15, 1513 (2011).
3. L. Kestens and S. Jacobs, *Texture, Stress Microstruct.* 173083, 1 (2008).
4. J.W. Morris, S.J. Hardy, and J.T. Thomas, *J. Mater. Process. Technol.* 120, 385 (2002).
5. H. Shimanaka, Y. Ito, K. Matsumara, and B. Fukuda, *J. Magn. Magn. Mater.* 26, 57 (1982).
6. Y. Oda, M. Kohno, and A. Honda, *J. Magn. Magn. Mater.* 320, 2430 (2008).
7. X. Wu, C. Gu, P. Yang, X. Gu, and S. Pang, *ISIJ Int.* 61, 1669 (2021).
8. J.Y. Park, K.H. Oh, and H.Y. Ra, *Scr. Mater.* 40, 881 (1999).
9. S. Da Costa Paolinelli, D. Cunha, and A. Cota, *Mater. Sci. Forum* 558, 787 (2007).
10. Y. He and E. Hilinski, *J. Magn. Magn. Mater.* 405, 337 (2016).
11. R. Kawamata, T. Kubota, and K. Yamada, *J. Mater. Eng. Perform.* 6, 701 (1997).
12. M. Mehdi, Y. He, E. Hilinski, L. Kestens, and A. Edrisy, *Acta Mater.* 185, 540 (2020).
13. K. Bourchas, A. Stening, J. Soulard, A. Broddefalk, M. Lindenmo, M. Dahlen, and F. Gyllensten, *IEEE Trans. Ind. Appl.* 53, 4269 (2017).
14. F. Humphreys and M. Hatherly, *Recrystallization and Related Annealing Phenomena*, 2nd edn. (Elsevier Ltd., New York, 2004), pp11–65.
15. T. Shimazu, M. Shiozaki, and K. Kawasaki, *J. Magn. Magn. Mater.* 133, 147 (1994).
16. J. Barros, A. Targhetta, O. León, T. Ros, J. Schneider, and Y. Houbaert, *J. Magn. Magn. Mater.* 316, e865 (2007).
17. M. Mehdi, Y. He, E. Hilinski, and A. Edrisy, *J. Magn. Magn. Mater.* 429, 148 (2017).
18. S.W. Cheong, E.J. Hilinski, and A.D. Rollett, *Metall. Mater. Trans. A* 34, 1311 (2003).
19. Y. He, T. Zhou, H. Lee, C. Cathcart, and P. Badgley, The Role of Temper Rolling and Annealing on the Magnetic Property Improvement of a Low Si Non-oriented Electrical Steel. Paper presented at the 152nd Annual Meeting & Exhibition (TMS 2023), San Diego, CA, USA, 19-23 March 2023.
20. ASTM International, "ASTM A726: Standard Specification for Cold-Rolled Magnetic Lamination Quality Steel, Semiprocessed Types", West Conshohocken, PA, 19428-2959 USA, 2018.
21. K.M. Lee, S.Y. Park, M.Y. Huh, J.S. Kim, and O. Engler, *J. Magn. Magn. Mater.* 354, 324 (2014).
22. C.P. Steinmetz, *Proc. IEEE* 72, 196 (1984).
23. J. Reinert, A. Brockmeyer, and R.W. De Doncker, *IEEE Trans. Ind. Appl.* 37, 1055 (2001).
24. H. Barkhausen, *Physikalishe Zeitschr* 20, 401 (1919).
25. C.G. Stefanita, *Chapter 2 Barkhausen Noise as a Magnetic Nondestructive Testing Technique*, ed. R. Hull, J.R.M. Osgood, J. Parisi, and J.H. Warlimont (Springer, Berlin, 2008), p. 19.
26. G. Bertotti, F. Fiorillo and G. P. Soardo, Journal de Physique, Vols. Colloque C8, Supplement au no 12, Tome 49, 1915 (1988).
27. C.D. Graham Jr., *J. Appl. Phys.* 53, 8276 (1982).
28. G. Bertotti, *IEEE Trans. Magn.* 24, 621 (1988).
29. S. Chikazumi and S.H. Charap, *Physics of Magnetism*, 2nd edn. (Oxford University, New York, 1997), pp299–339.

30. D.C. Jiles and D.L. Atherton, *J. Magn. Magn. Mater.* 61, 48 (1986).
31. D.C. Jiles and W. Kiarie, *IEEE Trans. Magn.* 57, 1 (2020).
32. M.J. Sablik, G.L. Burkhardt, H. Kwun, and D.C. Jiles, *J. Appl. Phys.* 63, 3930 (1988).
33. B.D. Cullity, *Introduction to Magnetic Materials*, 2nd edn. (Addison-Wesley, New York, 1972), pp197–239.
34. D.C. Jiles, *Introduction to Magnetism and Magnetic Materials* (Chapman and Hall, New York, 1991), pp69–86.
35. D. Utrata and M. Namkung, *Uniaxial Stress Effects on the Low-Field Magnetoacoustic Interactions in Low and Medium Carbon Steels*, Review of Progress in Quantitative Nondestructive Evaluation, Vol. 6B, ed. D. O. Thompson and D. E. Chimenti, (Plenum, Boston, New York, 1987), p. 1585.
36. D.C. Jiles, *NDT Int.* 21, 311 (1988).
37. D.J. Craik and R.S. Tebble, *Ferromagnetism and Ferromagnetic Domains*, 1st edn. (North Holland Publishing Co., Amsterdam, 1965).
38. M. P. Gallaugher, *The effect of easy axis orientation and misorientation on the magnetic properties of non-oriented electrical steels*. PhD Thesis, (McGill University, Montreal, 2015).
39. Y. Zhang, T. Yu, R. Xu, J. Thorborg, W. Liu, J. Tischler, A. Godfrey, and D.J. Jensen, *Mater Charact* 191, 112113 (2022).
40. G. Bertotti, G.D. Schino, A. Ferro, and F. Fiorillo, *J. De Physique* 46-C6, 385 (1985).
41. M. Shiozaki and Y. Kurosaki, *J. Mater. Eng.* 11, 37 (1989).
42. K.J. Overshott, *IEEE Trans. Magn.* 12, 840 (1976).
43. F.J.G. Landgraf, M. Emura, and M.F. de Campos, *J. Magn. Magn. Mater.* 320, e531 (2008).
44. W.A. Pluta, *Przegl*ąd Elektrotechniczny (Electrical Review) 87, 37 (2011).

Publisher's Note Springer Nature remains neutral with regard to jurisdictional claims in published maps and institutional affiliations.